Effective Field of a Dipole in Polarizable Fluids

E. L. Pollock and B. J. Alder
Lawrence Livermore Laboratory, University of California, Livermore, California 94550
(Received 24 May 1977)

The reaction field generated by a point dipole in a polarizable medium is considerably underestimated and the screening of the dipolar field is considerably overestimated by the classical continuum theory. The importance of the induced-dipole–induced-dipole contribution, particularly in reducing the screening in a normal liquid, is demonstrated by molecular-dynamics computer calculations.

Many physical situations require knowledge of the effective field at a dipole in a polarizable medium; for example, the difference between the dipole moment of a molecule in a fluid and in vacuum leads to an absorption frequency shift of a polar molecule when placed in solution.[1] The standard way to estimate this field is through the classical continuum theory of Onsager,[2] which embeds a point dipole in a spherical cavity surrounded by a homogeneous medium characterized by a dielectric constant. From this model the polarization which the dipole induces in its surroundings leads to a readily calculable field at the center called the reaction field and to a screened dipole field in the medium. It is the subject of this Letter to calculate this reaction field by rigorous statistical-mechanical methods and evaluate the accuracy of the continuum approximation. Of equal importance is a comparison of the screening of the dipole field by the induced polarization for large distances from the central dipole.

The test has been carried out for the simplest possible model in which a permanent point dipole $\vec{\mu}_0$, is surrounded by particles that have no permanent dipoles but only a point polarizability, α; in addition, all particles interact with the same short-ranged Lennard-Jones potential. The statistical-mechanical formulation of the effective electric field is straightforward,[3] and the field at particle j, at some distance away from the central dipole (labeled as 1), consists of two parts, the direct contribution from the permanent dipole and the induced contribution via all other particles k:

$$\vec{E}_j = \overleftrightarrow{T}_{j1}\cdot\vec{\mu}_0 + \sum_{k\neq 1}\overleftrightarrow{T}_{jk}\cdot\vec{p}_k, \tag{1}$$

where the induced dipole $\vec{p}_k = \alpha\vec{E}_k$ and $\overleftrightarrow{T}$ is the dipole-dipole tensor $\vec{\nabla}\vec{\nabla}(1/r)$. The reaction field or the field at the central dipole consists, of course, only of the induced part

$$\vec{E}_1 = \sum_{k\neq 1}\overleftrightarrow{T}_{1k}\cdot\vec{p}_k. \tag{2}$$

These equations can be solved iteratively, leading to an expansion in powers of α:

$$\vec{E}_j = \overleftrightarrow{T}_{j1}\cdot\vec{\mu}_0 + \alpha\sum_{k\neq 1,j}\overleftrightarrow{T}_{jk}\cdot\overleftrightarrow{T}_{k1}\cdot\vec{\mu}_0 + O(\alpha^2), \tag{3}$$

$$\vec{E}_1 = \alpha\sum_{k\neq 1}\overleftrightarrow{T}_{1k}\cdot\overleftrightarrow{T}_{k1}\cdot\vec{\mu}_0 + \alpha^2\sum_{k\neq 1}\sum_{j\neq 1,k}\overleftrightarrow{T}_{1k}\cdot\overleftrightarrow{T}_{kj}\cdot\overleftrightarrow{T}_{j1}\cdot\vec{\mu}_0 + O(\alpha^3). \tag{4}$$

These expressions have been evaluated analytically for hard spheres at low density to the order in α explicitly given. The linear term in the reaction field is easily reduced to[3] $\alpha A\vec{\mu}_0$, where

$$\vec{A} = 8\pi\rho\int dr\, g(r)/r^4, \tag{5}$$

with $g(r)$ the radial distribution function and ρ the number density. For low-density hard spheres of diameter σ, one gets $A = 8\pi\rho/3\sigma^3$. The linear screening term assumes the general asymptotic form

$$\sum_{k\neq 1,j}\overleftrightarrow{T}_{jk}\cdot\overleftrightarrow{T}_{k1} \to -\frac{4\pi}{3}\rho\overleftrightarrow{T}_{j1}, \tag{6}$$

which is exact for low-density hard spheres when $r_{1j}\geq 2\sigma$. The quadratic term in the reaction field is also calculable[4] so that

$$\vec{E}_j = (1 - 4\pi\rho\alpha/3)\overleftrightarrow{T}_{j1}\cdot\vec{\mu}_0 + O(\alpha^2) \quad \text{if} \quad r_{1j}\geq 2\sigma \tag{7}$$

and

$$\vec{E}_1 = \frac{8\pi\rho\alpha}{3\sigma^3}\vec{\mu}_0(1 - 5\pi\rho\alpha/8) + O(\alpha^3). \tag{8}$$

These low-density hard-sphere results should be directly comparable to the continuum-theory results since in both cases the structure of the

fluid is ignored. Thus, the Onsager model when applied to the present system predicts[5]

$$\vec{E}_j = 3\overleftrightarrow{T}_{j1}\cdot\vec{\mu}_0/(2\epsilon+1) \tag{9}$$

and

$$\vec{E}_1 = 2(\epsilon-1)\vec{\mu}_0/a^3(2\epsilon+1), \tag{10}$$

where a is the cavity radius. Substitution of the dielectric constant ϵ by the polarizability α, as given to high precision[6] by the Clausius-Mosotti equation

$$(\epsilon-1)/(\epsilon+2) = 4\pi\rho\alpha/3 + O(\alpha^3), \tag{11}$$

leads to

$$\vec{E}_j = (1-8\pi\rho\alpha/3)\overleftrightarrow{T}_{j1}\cdot\vec{\mu}_0 + (\alpha^2) \tag{12}$$

and

$$\vec{E}_1 = (8\pi\rho\alpha\mu_0/3a^3)(1-4\pi\rho\alpha/3) + O(\alpha^3), \tag{13}$$

where the $O(\alpha^3)$ corrections to the Clausius-Mosotti equation do not affect the terms given here. Thus, the continuum theory is only accurate to order α for the reaction field when a is identified with σ. To higher order, the continuum theory predicts a reaction field which is too small. On the other hand, the continuum theory overestimates by a factor of 2 the first-order screening term.

These rather large quantitative shortcomings of the continuum model are confirmed by the, in principle exact, molecular-dynamics calculations under various—including normal—liquid conditions. The equations of motion were solved including the dipole forces,[7] although for realistic values of the dipole moment and even for the largest value of the polarizability used, the dipole forces did not significantly affect the structure of the fluid. (See the radial distribution functions presented below as evidence.) Note also that since the dipole–induced-dipole forces fall off faster than $1/r^3$, this calculation is not plagued by boundary-condition problems due to long-range forces. Hence periodic-boundary conditions were employed for the dynamics with the modification that the image particles have no dipole moment. The polarization was confined to the largest sphere that could be contained within the periodic box around the central permanent dipole, which was arbitrarily fixed along the z axis. At each time step the self-consistent electric field was calculated iteratively starting from the field and polarization of the previous step. Convergence was assumed when the electric field energy was constant to better than 1 part in 10^4. The first-order field E^1 is obtained in a separate calculation by a single iteration starting from the unscreened field for comparison with the theory. The problem was run on a parallel-processing computer, CDC STAR, in vector mode, for which this kind of calculation is particularly well suited, with an accuracy in the energy to better than 1 part in 10^4.

The results for the reaction field at several densities and temperatures are summarized in Table I. Evaluation of the integral[8] in Eq. (5) leads to agreement with the term linear in α, $E_1{}^1$, and serves as an independent verification of the numerical procedure. The new results are given by the sum of all further iterations, labeled $E_1{}^R$. They lead to a decrease of the reaction field by about 10% for a liquid like xenon ($\alpha/\sigma^3 = 0.06$) at the normal boiling point. As expected, these

TABLE I. Results for the reaction field. In all calculations 108 particles were used except the two cases marked with an asterisk, where 256 particles were used. Runs were typically 40 000 time steps long. The time step is the same as in the usual Lennard-Jones calculation. Error estimates are typically 1 in the last significant figure given. The central dipole had a value of $\mu_0/(\epsilon_{LJ}\sigma^3)^{1/2} = 1$, where ϵ_{LJ} is the depth of the intermolecular potential and σ is the distance at which the intermolecular potential crosses the zero axis.

$\rho\sigma^3$	kT/ϵ_{LJ}	α/σ^3	ϵ	$E_1{}^1$	$-E_1{}^R$	a_0	a_w	σ_e
0.84	0.80	0.14	3.94	1.66	0.256	0.78	0.87	0.98
0.84*	0.67	0.10	2.64			0.77	0.83	0.98
0.84*	0.72	0.05	1.64	0.58	0.051	0.83	0.86	0.98
0.84	0.70	0.02	1.23	0.23	0.009	0.84	0.85	0.98
0.70	1.97	0.10	2.24			0.78	0.82	0.96
0.20	2.01	0.10	1.27	0.24	0.007	0.87	0.89	0.96

higher-order contributions become smaller as α and the density become smaller. The value of a_0 given in Table I signifies the radius of the cavity that has to be introduced in the Onsager expression for the reaction field in order to reproduce the computer results. Similarly a_w is such a radius for a recently proposed alternative theory.[9] These very similar values must be compared to the considerably larger values of the equivalent hard-sphere diameter, σ_e, for the Lennard-Jones potential that one would have thought appropriate, since these can be used to describe accurately the thermodynamic properties.[10] Since these diameters are cubed, the continuum theory can be seen to underestimate the reaction field considerably.

The separate contributions to the screening are shown in Fig. 1. The first-order contribution E_j^1 is shown as projected in the fixed direction of the permanent dipole

$$E_j^1(r) = \int E_j^1(\vec{r}) P_2(\cos\theta)\, d\Omega. \qquad (14)$$

The first-order contribution is normalized by its previously established asymptotic limit at large separation $-\frac{4}{5}(4\pi\rho\alpha\mu_0/3r^3)$, where the $\frac{4}{5}$ factor derives from the projection. This first-order normalized screening, $S^1(r)$, is shown in the lower part of Fig. 1 to approach the correct theoretical limit at large distances, indicating that the machine calculations have been carried out to distances beyond which the structure of the fluid can be ignored. Furthermore, at small distances between particle j and the central dipole 1 the screening, as expected, vanishes. The screening contribution of all higher terms beyond the first $S^R(r)$, again projected and normalized by the same factor as $S^1(r)$, is shown in the upper part of Fig. 1. The induced-dipole–induced-dipole contributions, $S^R(r)$, are seen always to decrease the screening, increasingly so for larger α values. In the case of liquid xenon, the decrease amounts to about 20% at large distances.

The effective screening, from which an effective dielectric constant as a function of distance from the central dipole could be readily deduced, is shown in Fig. 2. The effective screening $S^R(r)$ is again the projected dipolar part of $E_j(\vec{r})$ but this time normalized by the projected unscreened dipole field $4\mu_0/5r^3$. The screening factors of the continuum theory are shown by the dashed lines for the two different values of the polarizability and are seen to predict much too high a screening. At the lower value of the polarizability, this is primarily due to the factor-of-2 discrepancy pointed out above. However, for the large polarizability value, the higher-order induced terms also make a significant contribution so that the resulting dipolar field is nearly unscreened. In fact, at sufficiently high values of the polarizability ($\alpha/\sigma^3 \gtrsim 0.2$), these higher-order terms lead to a "polarization catastrophe" or spontaneous polarization of the surroundings. Finally, it should be noted from Fig. 2 that the effective screening at intermediate distances shows a

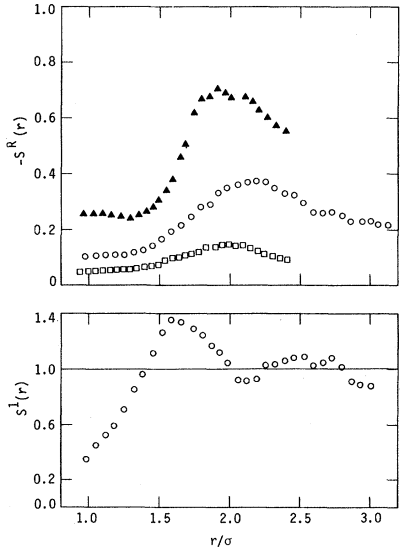

FIG. 1. The first-order screening contribution, $S^1(r)$, and all higher-order contributions, $S^R(r)$, as a function of the reduced distance from the central dipole r/σ. The conditions correspond to the first (triangles), third (circles), and fourth (squares) entries in Table I.

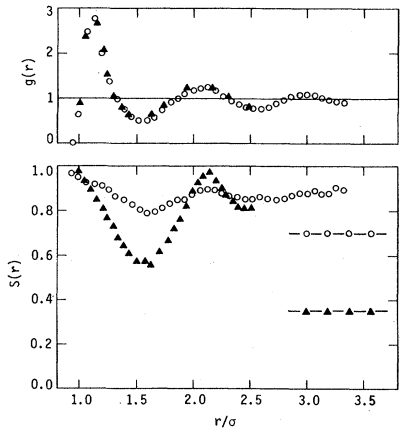

FIG. 2. The effective screening factor for the dipole field, $S(r)$, and the radial distribution function $g(r)$ for the same conditions as those symbolized in Fig. 1. The dashed-symbol lines indicate the continuum-model results.

structure which is closely related to that of the radial distribution function.

This work was performed under the auspices of the U. S. Energy Research and Development Administration under Contract No. W-7405-Eng-48.

[1]D. E. Sullivan and J. M. Deutch, J. Chem. Phys. 66, 5315 (1977).
[2]L. Onsager, J. Am. Chem. Soc. 58, 1486 (1936).
[3]J. G. Kirkwood, J. Chem. Phys. 4, 592 (1936).
[4]G. Casanova *et al.*, Mol. Phys. 18, 589 (1970).
[5]H. Fröhlich, *Theory of Dielectrics* (Oxford Univ. Press, Londin, 1949).
[6]B. J. Alder, H. L. Strauss, and J. J. Weiss, J. Chem. Phys. 62, 2328 (1975).
[7]F. J. Vesely, to be published.
[8]G. Stell, J. C. Rasaiah, and H. Narang, Mol. Phys. 23, 393 (1972).
[9]M. S. Wertheim, Mol. Phys. 25, 211 (1973).
[10]J. A. Barker and D. Henderson, J. Chem. Phys. 47, 4714 (1967).

Thermally Induced Breakdown of the Direct-Transition Model in Copper

R. S. Williams, P. S. Wehner, J. Stöhr, and D. A. Shirley
Materials and Molecular Research Division, Lawrence Berkeley Laboratory, and Department of Chemistry, University of California, Berkeley, California 94720
(Received 19 April 1977)

A strong temperature dependence has been observed for the first time in angle-resolved photoemission (ARP) spectra of the valence band of a crystalline solid. This spectral behavior confirms predictions of a model suggested by Shevchik. A controversial point in the interpretation of ARP spectra at x-ray energies is resolved by this model. Moreover, it dictates the choice of photon energy and sample temperature for future ARP studies of valence-band electronic structure.

Shevchik[1] has suggested that thermal broadening leads to a more complete sampling of the first Brillouin zone (BZ) in angle-resolved x-ray photoemission than would be expected from a rigorous direct-transition model. He expressed the angle-resolved photoemission cross section as the sum of a k-conserving direct-transition term and an atomic term, with the relative contributions of the two being governed by the Debye-Waller factor, which we shall write as

$$f = \exp[-\langle(\vec{q}\cdot\Delta\vec{r}_T)^2\rangle], \tag{1}$$

where $\vec{q}=\vec{k}_f-\vec{k}_i-\vec{k}_{h\nu}$ ($\vec{k}_f$ and $\vec{k}_i$ are the final and initial electron momentum and $\vec{k}_{h\nu}$ is the photon momentum) and $\Delta\vec{r}_T$ is the instantaneous thermal displacement of an atom in the lattice.

The energy distribution function for photoelectrons *inside* a crystal is given by[2]

$$N(E_f,\vec{k}_f,h\nu)\propto\sum_{\vec{k}_i}^{\vec{k}_i\subset \mathrm{BZ}}\sum_{E_j(\vec{k}_i)}^{E_j<E_F}|\langle E_f(\vec{k}_f)|\vec{A}\cdot\vec{p}|E_j(\vec{k}_i)\rangle|^2\delta[E_f(\vec{k}_f)-E_j(\vec{k}_i)-h\nu]. \tag{2}$$

where the summations are over the initial momentum states ($\vec{k}_i$) in the first BZ and all occupied energy levels. If electron transport and surface transmission do not alter N significantly, an experimental energy distribution curve (EDC) can be obtained by summing Eq. (2) over the final energy and momentum states (E_f and $\vec{k}_f$) allowed by the finite angular resolution of the measurement and the uncertainty in the component of crystal momentum perpendicular to the sample surface. If we assume a tight-binding initial state and plane-wave final state,[3] the matrix element of Eq. (2) demonstrates a temperature dependence similar to x-ray diffuse scattering theory[4]; i.e.,

$$|\langle\exp(i\vec{k}_f\cdot\vec{r})|\vec{A}\cdot\vec{p}|E_j(\vec{k}_i)\rangle|^2$$
$$\propto\cos^2\gamma f\sigma_{ij}(\vec{k}_f)\{\delta(\vec{q}-\vec{G})+[1-\delta(\vec{q}-\vec{G})][k_BT(|\vec{q}|^2/|\vec{q}-\vec{G}|^2)\varphi_1+(k_BT)^2|\vec{q}|^4\varphi_2(\vec{q})+\ldots]\}. \tag{3}$$

Here γ is the angle between the electric field polarization vector and $\vec{k}_f$, $\sigma_{ij}(\vec{k}_f)$ is the atomic cross section,[5] $\vec{G}$ is a reciprocal-lattice vector, k_B is the Boltzmann constant, and φ_1 and $\varphi_2(\vec{q})$ involve sums